ACS central science

A Mitochondrial-Targeted Nitroxide Is a Potent Inhibitor of Ferroptosis

Tanja Krainz,[†] Michael M. Gaschler,[§] Chaemin Lim,[†] Joshua R. Sacher,[†] Brent R. Stockwell,*[‡,§] and Peter Wipf*[†]

[†]Department of Chemistry, University of Pittsburgh, 219 Parkman Avenue, Pittsburgh, Pennsylvania 15260, United States
[‡]Department of Biological Sciences and [§]Department of Chemistry, Columbia University, 550 West 120th Street, Northwest Corner Building, MC 4846, New York, New York 10027, United States

ⓈSupporting Information

ABSTRACT: Discovering compounds and mechanisms for inhibiting ferroptosis, a form of regulated, nonapoptotic cell death, has been of great interest in recent years. In this study, we demonstrate the ability of XJB-5-131, JP4-039, and other nitroxide-based lipid peroxidation mitigators to prevent ferroptotic cell death in HT-1080, BJeLR, and panc-1 cells. Several analogues of the reactive oxygen species (ROS) scavengers XJB-5-131 and JP4-039 were synthesized to probe structure–activity relationships and the influence of subcellular localization on the potency of these novel ferroptosis suppressors. Their biological activity correlated well over several orders of magnitude with their structure, relative lipophilicity, and respective enrichment in mitochondria, revealing a critical role of intramitochondrial lipid peroxidation in ferroptosis. These results also suggest that preventing mitochondrial lipid oxidation might offer a viable therapeutic opportunity in ischemia/reperfusion-induced tissue injury, acute kidney injury, and other pathologies that involve ferroptotic cell death pathways.
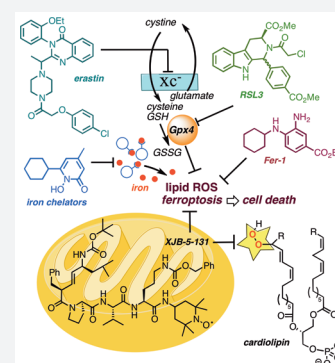
Cell death can be broadly divided into two major categories: uncontrolled cell death that arises from overwhelming cellular injury and regulated cell death that relies on tightly controlled molecular pathways. Apoptosis is the most characterized form of regulated cell death, initiating cell death by activating caspases. Yet, in addition to apoptosis, other types of regulated cell death have recently been discovered.[1,2] Ferroptosis is an oxidative, nonapoptotic form of regulated cell death characterized by the iron-dependent accumulation of lipid peroxides.[3] Lipophilic antioxidants and iron chelators, but not caspase inhibitors, can effectively inhibit ferroptosis. While mechanistic information is still emerging, the selenoprotein glutathione peroxidase 4 (Gpx4)[4] is the master regulator of ferroptosis, controlling lipid peroxide formation (Figure 1).[5,6] Under low glutathione (GSH) conditions, Gpx4 is unable to reduce lipid hydroperoxides. A combination of lipoxygenase and ROS-mediated phospholipid oxidations then causes ferroptotic cell death.[7] Isoforms of Gpx4 exist in the cytosol, nucleus, and mitochondria, and the primary subcellular origin of lethal lipid peroxide formation is not yet known. While the development of inhibitors and promoters of ferroptosis is currently under active investigation due to their potential therapeutic opportunities, there is still an urgent need to develop chemical probes that elucidate mechanistic details of this new biological pathway.[2,8,9]

Since ferroptosis is accompanied by a burst in lipid peroxidation,[10] we hypothesized that a mitochondrially targeted nitroxide such as XJB-5-131, or a more broadly intracellularly distributed antioxidant, JP4-039, might be effective inhibitors of this cell death pathway. Furthermore, the different levels of

mitochondrial enrichment of these two agents would allow us to differentiate the relative contribution of mitochondrial versus extramitochondrial lipid peroxidation in ferroptosis.[11−15] The alkene peptide isostere moiety and the type II′ β-turn structure of XJB-5-131 are responsible for its ca. 600-fold enrichment in the mitochondria over the cytosol.[10] JP4-039 contains a nitroxide attached directly to the alkene-peptide isostere, and compared to the parent molecule XJB-5-131, this truncated analogue benefits from lower molecular weight, logP, polar surface area, and higher aqueous solubility (Figure 2). JP4-039 retains many of the desired physiological effects of XJB-5-131, including radiation damage prevention and mitigation; however, it only displays a 20−30-fold enrichment in mitochondria over the cytosol.[10] Both nitroxides have demonstrated impressive biological activity in *in vitro* and *in vivo* models of diseases related to reactive oxygen species formation, and previous studies have highlighted their mechanism of action and therapeutic potential.[16−19]

In this study, we investigated the ability of XJB-5-131, JP4-039, and selected analogues to prevent ferroptosis in human HT-1080, BJeLR, and panc-1 cells to determine the role of intramitochondrial lipid peroxidation in ferroptosis. Several novel analogues of XJB-5-131 and JP4-039 were synthesized to probe structure−activity relationships (SARs) and the influence of the relative subcellular localization of the nitroxides.
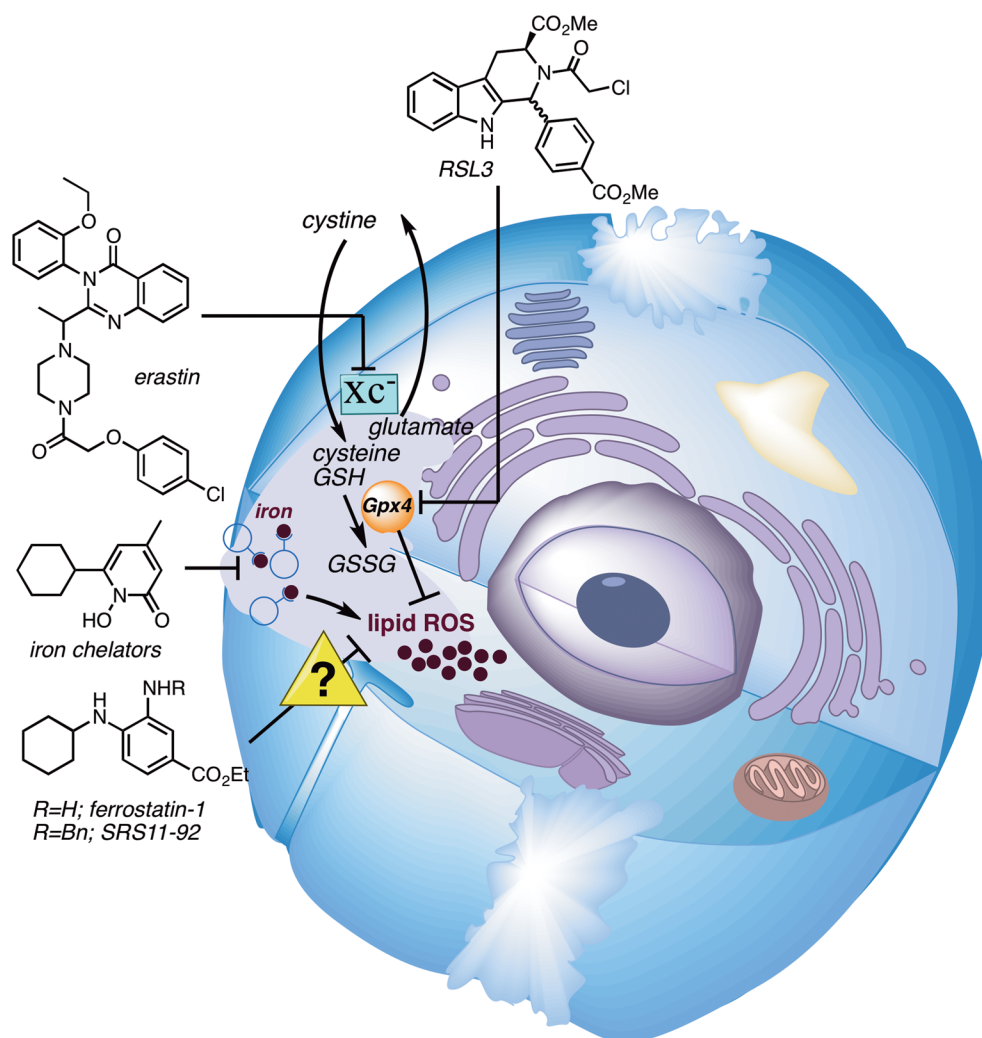
Figure 1. Iron-dependent lipid peroxidation is a hallmark of ferroptosis, which is triggered by inhibition of the glutamate-cysteine antiporter system (system X_c^-) with erastin or inhibition of Gpx4 with RSL3. Iron chelators and lipophilic antioxidants, such as ferrostatin-1 and SRS11-92, prevent ferroptosis.
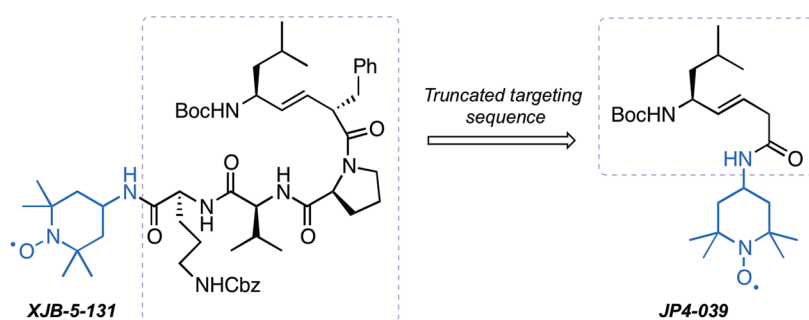
Figure 2. Structures of XJB-5-131 and JP4-039; the mitochondrial targeting sequences are highlighted in a dashed box; the nitroxide payload shown in blue provides effective scavenging of reactive oxygen species (ROS), organic radicals, and electrons escaping from the electron transfer chain (ETC).

Initially, ferroptosis sensitive HT-1080 fibrosarcoma cells were treated with a lethal dose of erastin (10 μM) or RSL3 (2 μM) and varying concentrations of XJB-5-131, JP4-039, or the validated ferroptosis inhibitor ferrostatin-1 (Fer-1).[3] XJB-5-131 showed low nanomolar potency against both ferroptosis inducers; this highly targeted nitroxide had potency similar to that of Fer-1 against erastin, but was 5-fold less protective against RSL3 (Figure 3 and Table 1). In contrast, JP4-039 was much less protective than Fer-1 or XJB-5-131, and the difference in potency, ca. 20- to 30-fold against both ferroptosis inducers, was in excellent agreement with the relative enrichment of these two lipid peroxidation inhibitors in mitochondria (a 20–30- vs 600-fold preference for the mitochondrial vs cytosolic cell fraction for JP4-039 and XJB-5-131, respectively).
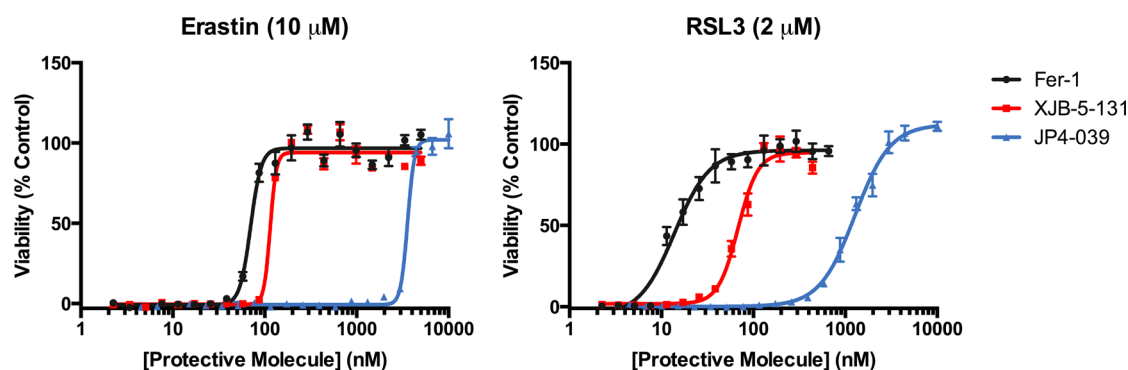
Figure 3. Protective effects of XJB-5-131 and JP4-039 in HT-1080 cells against erastin-induced and RSL3-induced ferroptosis.

Table 1. Protective Effects of XJB-5-131 and JP4-039 in HT-1080 Cells against Erastin-Induced and RSL3-Induced Ferroptosis

| entry | analogue | logP[20] | EC_{50} [95% confidence interval] (nM) | |
			erastin	(1S,3R)-RSL3
1	Fer-1	2.8	70 [66−73]	13 [12−15]
2	XJB-5-131	6.1	114 [104−125]	68 [64−72]
3	JP4-039	2.9	3580 [3471−3692]	1274 [1203−1350]

These initial studies supported a hypothesis that ferroptosis is intrinsically linked to a lipid oxidation pathway intersecting with the mitochondrial membrane, since XJB-5-131 strongly suppresses cardiolipin-derived oxidized fatty acid formation.[11,16] In order to demonstrate that this effect was tractable and dependent on the structure of the mitochondrial-targeting sequence in the XJB and JP4 series, which correlates to their relative enrichment in mitochondria, we synthesized and tested a series of analogues of both XJB-5-131 and JP4-039 (Schemes 1 and 2).

Cleavage of the Boc function of XJB-5-131 with trifluoroacetic acid (TFA) and introduction of a solubilizing oxetanyl sulfoxide with the activated carbonate 1[21,22] provided a less lipophilic analogue 2 (logP[20] 5.2 vs 6.1 for XJB-5-131). Boc deprotection of 3 followed by coupling to acid 4[10] provided methyl ester 5 in 86% yield over 2 steps. Subsequent hydrolysis and coupling to 4-amino-TEMPO (4-AT) provided nitroxide 6. By virtue of the oxetanyl sulfoxide side chain, analogue 2 demonstrated significantly improved water solubility over the parent XJB-5-131 (150 vs 1200 μg/mL). A consequence of this structural change was an expected decrease in affinity for lipid membranes, and indeed with an EC_{50} of 3.5 μM, a 30-fold loss in activity was detected for 2 vs XJB-5-131 (Figure 4 and Table 2). In contrast, shortening the C-terminal sequence of XJB-5-131 by one amino acid residue (e.g., the side-chain Cbz-protected ornithine) led only to a 4-fold decrease in activity to an EC_{50} of 465 nM observed for analogue 6, demonstrating that the biological activity is sequence-dependent and not just lipophilicity-dependent, since 2 and 6 have identical logP values of 5.2.

A D-amino acid residue at the (i+1)-position in a tetrapeptide sequence strongly stabilizes a type II′ β-turn, a conformation that is known to improve permeability through membranes.[23−25] The D-phenylalanine-L-proline moiety together with the (E)-alkene isostere in XJB-5-131 therefore facilitate the formation of a compact structure that maximizes intramolecular hydrogen bonding even in a protic environment and

promote permeability either due to the nature of the folded structure itself or because the folded conformation is an energetically favorable precursor to the preferentially permeable structure.[26,27] Accordingly, we speculated that removal of the benzyl side chain on XJB-5-131 would significantly increase the number of conformational isomers by eliminating a backbone constraint, and reduce its antiferroptotic properties by lowering its concentration in the mitochondrial membrane. The preparation of the truncated analogues 10 and 11 that tested this hypothesis was achieved in 3 and 5 steps, respectively, from the previously described β,γ-unsaturated acid 8, which was accessible in 7 steps and 73% overall yield from 3-butyn-1-ol.[28] Pentapeptide 9 was obtained from a coupling of acid 8 and tripeptide H-Pro-Val-Orn(Cbz)-OMe. Subsequent hydrolysis of the methyl ester followed by coupling to 4-AT provided the debenzylated alkene peptide isostere 10, which was converted to an additional analogue by the removal of the Boc protecting group and N-acylation with 1 to give oxetane 11 in 83% yield over the 2 steps. The effect of the removal of the D-amino acid backbone constraint in the β-turn was indeed significant, since the EC_{50} of 895 nM of analogue 10 established it to be about 8-fold less effective than XJB-5-131, and analogue 11 failed to demonstrate any inhibitory activity against erastin-induced ferroptosis below the 10 μM concentration cutoff.

Overall, the SAR of analogues 2, 6, 10, and 11 of the highly mitochondrially targeted XJB-5-131 supported our fundamental hypothesis that mitochondrial lipid oxidation is critical in promoting the ferroptotic cell death pathway, and that effective inhibitors of this process needed to be primarily localized to mitochondria in order to have significant potency. For additional control experiments, we also performed structural modifications on the less targeted, but still active, JP4-039 and recorded their effects on the prevention of erastin-induced ferroptosis.

Nitroxides 13a−d were synthesized via a three-step sequence involving reduction of the nitroxide to the hydroxylamine, Boc deprotection of JP4-039, and coupling to the activated ester 12 containing a substituted oxetane in 55−60% overall yields (Scheme 2). We also removed the carbamate side chain and prepared a more hydrophilic oxetanylamine, 16 (logP 1.7), by reductive amination with ketone 15. Analogous to the results obtained with 2 and 11, the replacement of the Boc group by a hydrophilic oxetane-containing side chain was not tolerated, and all modified analogues 13a−d of JP4-039 lost activity. In this series, we also experimented with the introduction of a second nitroxide on the backbone alkene isostere, which should double the antiferroptotic effect in a stoichiometric mode, theoretically lowering the EC_{50} of JP4-039 from 3.6 μM to ca.

**Scheme 1. Synthesis of Backbone- and Side-Chain-Modified Analogues of XJB-5-131**
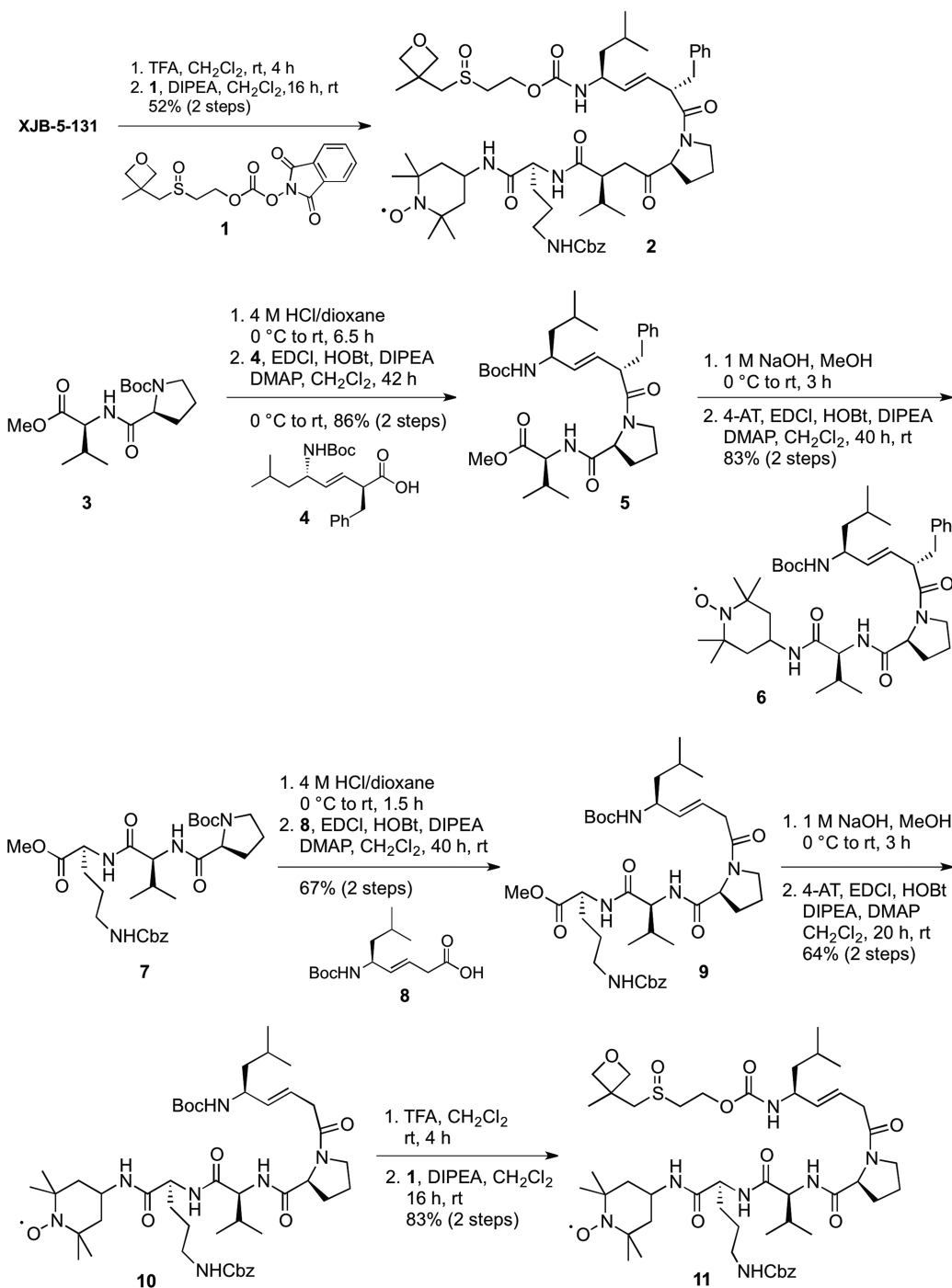
1.5–2 μM. Bisnitroxide **18** was obtained in 56% yield by acylation of the trifluoroacetate salt of *N*-deprotected JP4-039 with activated carbonate **17**. This compound had an EC₅₀ of 915 nM in erastin-treated cells, in agreement with our hypothesis that a doubling in nitroxide content while maintaining the backbone sequence would improve the ability of this particular scaffold to scavenge ROS responsible for promoting ferroptosis, irrespective of the slightly lower logP of **18** vs JP4-039.

To confirm these observations in additional cell lines, we tested the active compounds in ferroptosis sensitive BJeLR and panc-1 cells (Figure S1). While there was some variability in the potency of active compounds between cell lines, the general

trends of potency observed in HT-1080 cells were consistent among all other cell lines tested. XJB-5-131 was consistently the most potent nitroxide at a level similar to that of ferrostatin-1. JP4-039 remained ca. 10–20-fold less protective than XJB-5-131 in both cell lines when treated with erastin or RSL3. These data demonstrate that mitochondria-targeted nitroxides are able to inhibit ferroptosis in a variety of tissue types and across multiple growth conditions.

To determine whether XJB and ferrostatin acted synergistically or additively, we further tested the combination of these two inhibitors (Figure S2). HT-1080 cells were treated with a lethal dose of erastin and either XJB-5-131, ferrostatin-1, or both at concentrations below their EC₅₀. Cotreatment of HT-

Scheme 2. Synthesis of Backbone- and Side-Chain-Modified Analogues of JP4-039
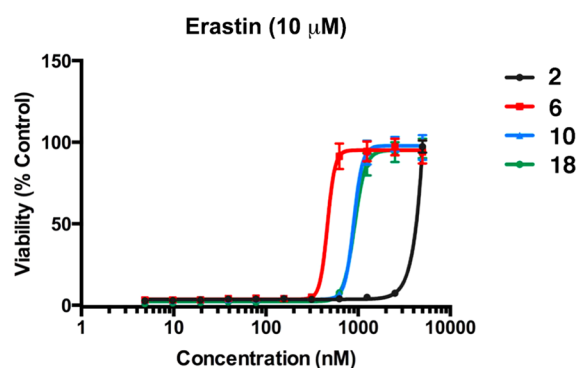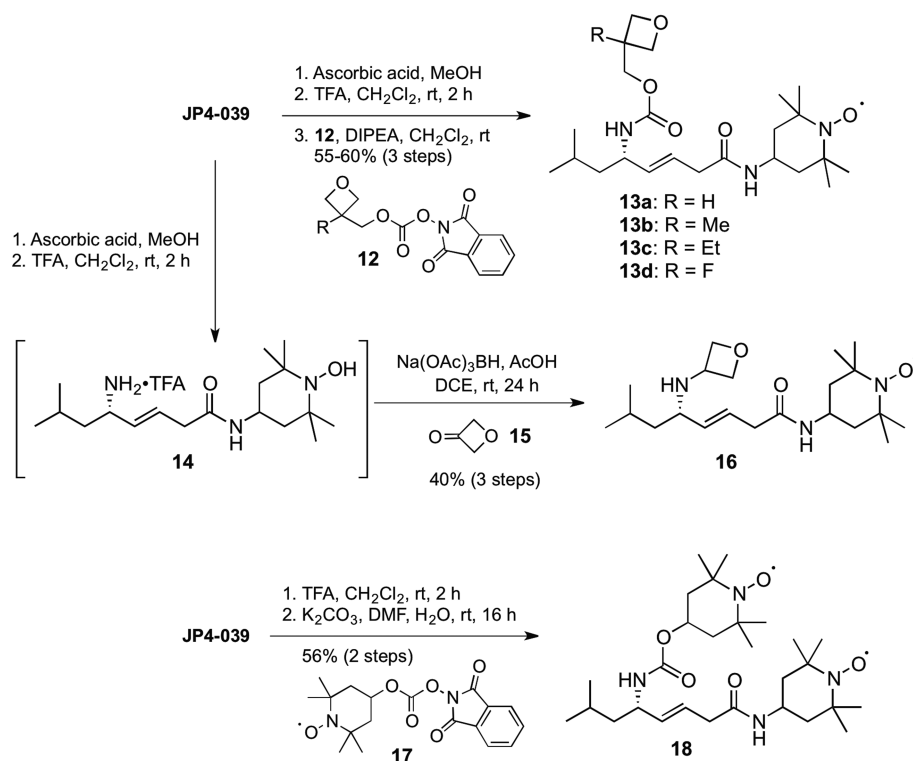
Figure 4. Protective effects of XJB-5-131 and JP4-039 analogues to prevent erastin-induced ferroptosis in HT-1080 cells.

Table 2. Protective Effects of XJB-5-131 and JP4-039 Analogues To Prevent Erastin-Induced Ferroptosis in HT-1080 Cells

entry	analogue	logP[20]	EC$_{50}$ [95% confidence interval] (nM) in HT-1080 cells
1	2	5.2	3478 [3375−3583]
2	6	5.2	465 [413−524]
3	10	4.1	895 [836−958]
4	11	2.0	>10 000
5	13a−d	1.7 to 2.6	>10 000
6	16	1.7	>10 000
7	18	2.6	915 [871−960]

1080 cells with ferrostatin-1 and XJB-5-131 did not produce a significant increase in viability compared to treatment with ferrostatin-1 alone. These data suggest that ferrostatin-1 and XJB-5-131 may share similar mechanisms of action or that both compounds operate on the same signaling pathway.

Ferroptosis has been implicated in a number of degenerative pathologies,[10] and the identification of inhibitors of ferroptosis is therefore of translational interest. Our finding that mitochondrially targeted nitroxides based on the XJB-5-131 lead structure are potent suppressors of ferroptosis in multiple cell contexts suggests that such compounds might be effective in treating degenerative diseases involving ferroptosis. Although the ADME properties of this series need to be evaluated and likely optimized,[29] the results reported herein suggest a new approach to creating drugs that inhibit ferroptosis.

On the other hand, inducing ferroptosis may be a useful approach to treating some sensitive cancers.[10] One concern in this regard is that ferroptosis inhibitors such as XJB-5-131 might promote growth or persistence of certain tumors that would not otherwise survive. It will clearly be important to determine to what extent inhibitors of ferroptosis have the ability to promote tumor formation, and to what extent inducers of ferroptosis may trigger degenerative pathologies.

Prior mechanistic studies of ferroptosis had provided data that were simultaneously both supporting and opposing the hypothesis that mitochondrial lipid peroxidation is required for ferroptotic cell death. In support of this hypothesis was the observation that the major morphological change in erastin-treated cells is the degeneration of mitochondria.[30] Additionally, Gpx4 knockout kidneys show an accumulation of oxidized cardiolipin, a mitochondria-specific phospholipid; this was particularly intriguing in light of the ability of XJB-5-131 to suppress oxidation of cardiolipin.[7] Opposing this hypothesis were the observations that (i) the mitochondrial electron transport chain is not needed for erastin-induced ferroptosis,[3] (ii) the mitochondrially targeted superoxide probe MitoSOX is not oxidized in erastin-treated cells,[31] (iii) the ferroptosis inhibitor ferrostatin-1 does not suppress rotenone-induced MitoSOX oxidation, which is likely due to mitochondrial

complex I derived superoxide,[30] and (iv) ferrostatin does not suppress the staurosporine-induced decrease in the 10-nonyl acridine orange (NAO) signal.[30] Nonetheless, these previous observations are not inconsistent with a role for mitochondrial lipid peroxidation in ferroptosis if superoxide is not involved, and if NAO does not report specifically on mitochondrial lipid peroxidation. Thus, given that these earlier mechanistic probes are indirect and potentially nonspecific reporters of mitochondrial lipid peroxidation, we reasoned that testing a mitochondrially targeted nitroxide would be a more effective means of examining the hypothesis that mitochondrial lipid peroxidation is a necessary condition for ferroptosis. Our results with a series of mitochondrially targeted nitroxides as lipid peroxidation mitigators indicate that the protection of mitochondrial lipids is sufficient for prevention of ferroptosis, and that untargeted ROS scavenging in the cytosol has relatively minor, if any, significance for the induction or propagation of this cell death pathway. While it is still premature to conclude that disruption of mitochondrial Gpx4 activity is a more critical contributor to ferroptosis than the cytosolic or nuclear Gpx4 isoforms are, our new results would be in agreement with such a revised mechanistic hypothesis. Undoubtedly, however, these studies highlight that mitochondrial lipid peroxidation is a key factor in ferroptosis, and preventing such lipid peroxidation in mitochondrial membranes is likely to be therapeutically relevant in diseases where ferroptotic cell death plays a major role.

■ ASSOCIATED CONTENT

Ⓢ Supporting Information

The Supporting Information is available free of charge on the ACS Publications website at DOI: 10.1021/acscentsci.6b00199.

Experimental procedures and spectroscopic data (PDF)

■ AUTHOR INFORMATION

Corresponding Authors
*E-mail: bstockwell@columbia.edu.
*E-mail: pwipf@pitt.edu.

Notes
The authors declare the following competing financial interest(s): P.W. is a cofounder of Solano, a company interested in the development of drugs for the treatment of neurodegenerative diseases, and listed as an inventor on patents assigned to the University of Pittsburgh that cover certain targeted nitroxides.

■ ABBREVIATIONS

4-AT, 4-amino-TEMPO; DIPEA, diisopropylethylamine; DMAP, 4-dimethylaminopyridine; EDCl, 1-ethyl-3-(3-(dimethylamino)propyl)carbodiimide; HOBt, 1-hydroxybenzotriazole; ROS, reactive oxygen species; SAR, structure−activity relationship; TFA, trifluoroacetic acid; Fer-1, ferrostatin-1

■ REFERENCES

(1) Aki, T.; Funakoshi, T.; Uemura, K. Regulated necrosis and its implications in toxicology. *Toxicology* **2015**, *333*, 118−126.

(2) Conrad, M.; Friedmann Angeli, J. P.; Vandenabeele, P.; Stockwell, B. R. Regulated necrosis: disease relevance and therapeutic opportunities. *Nat. Rev. Drug Discovery* **2016**, *15*, 348−366.

(3) Dixon, S. J.; Lemberg, K. M.; Lamprecht, M. R.; Skouta, R.; Zaitsev, E. M.; Gleason, C. E.; Patel, D. N.; Bauer, A. J.; Cantley, A. M.; Yang, W. S.; Morrison, B.; Stockwell, B. R. Ferroptosis: An iron-dependent form of nonapoptotic cell death. *Cell* **2012**, *149*, 1060−1072.

(4) Conrad, M.; Friedmann Angeli, J. P. Glutathione peroxidase 4 (Gpx4) and ferroptosis: What's so special about it? *Mol. Cell. Oncol.* **2015**, *2*, e995047.

(5) Dixon, S. J.; Stockwell, B. R. The role of iron and reactive oxygen species in cell death. *Nat. Chem. Biol.* **2014**, *10*, 9−17.

(6) Yang, W. S.; SriRamaratnam, R.; Welsch, M. E.; Shimada, K.; Skouta, R.; Viswanathan, V. S.; Cheah, J. H.; Clemons, P. A.; Shamji, A. F.; Clish, C. B.; Brown, L. M.; Girotti, A. W.; Cornish, V. W.; Schreiber, S. L.; Stockwell, B. R. Regulation of ferroptotic cancer cell death by Gpx4. *Cell* **2014**, *156*, 317−331.

(7) Friedmann Angeli, J. P.; Schneider, M.; Proneth, B.; Tyurina, Y. Y.; Tyurin, V. A.; Hammond, V. J.; Herbach, N.; Aichler, M.; Walch, A.; Eggenhofer, E.; Basavarajappa, D.; Rådmark, O.; Kobayashi, S.; Seibt, T.; Beck, H.; Neff, F.; Esposito, I.; Wanke, R.; Förster, H.; Yefremova, O.; Heinrichmeyer, M.; Bornkamm, G. W.; Geissler, E. K.; Thomas, S. B.; Stockwell, B. R.; O'Donnell, V. B.; Kagan, V. E.; Schick, J. A.; Conrad, M. Inactivation of the ferroptosis regulator Gpx4 triggers acute renal failure in mice. *Nat. Cell Biol.* **2014**, *16*, 1180−1191.

(8) Abrams, R. P.; Carroll, W. L.; Woerpel, K. A. Five-membered ring peroxide selectively initiates ferroptosis in cancer cells. *ACS Chem. Biol.* **2016**, *11*, 1305−1312.

(9) Xie, Y.; Song, X.; Sun, X.; Huang, J.; Zhong, M.; Lotze, M. T.; Zeh, H. J.; Kang, R.; Tang, D. Identification of baicalein as a ferroptosis inhibitor by natural product library screening. *Biochem. Biophys. Res. Commun.* **2016**, *473*, 775−780.

(10) Yang, W. S.; Stockwell, B. R. Ferroptosis: death by lipid peroxidation. *Trends Cell Biol.* **2016**, *26*, 165−176.

(11) Wipf, P.; Xiao, J.; Jiang, J.; Belikova, N. A.; Tyurin, V. A.; Fink, M. P.; Kagan, V. E. Mitochondrial targeting of selective electron scavengers: Synthesis and biological analysis of hemigramicidin-tempo conjugates. *J. Am. Chem. Soc.* **2005**, *127*, 12460−12461.

(12) Jiang, J.; Kurnikov, I.; Belikova, N. A.; Xiao, J.; Zhao, Q.; Amoscato, A. A.; Braslau, R.; Studer, A.; Fink, M. P.; Greenberger, J. S.; Wipf, P.; Kagan, V. E. Structural requirements for optimized delivery, inhibition of oxidative stress, and antiapoptotic activity of targeted nitroxides. *J. Pharmacol. Exp. Ther.* **2007**, *320*, 1050−1060.

(13) Jiang, J.; Belikova, N. A.; Hoye, A. T.; Zhao, Q.; Epperly, M. W.; Greenberger, J. S.; Wipf, P.; Kagan, V. E. A mitochondria-targeted nitroxide/hemigramicidin S conjugate protects mouse embryonic cells against gamma irradiation. *Int. J. Radiat. Oncol., Biol., Phys.* **2008**, *70*, 816−825.

(14) Rwigema, J.-C. M.; Beck, B.; Wang, W.; Doemling, A.; Epperly, M. W.; Shields, D.; Goff, J. P.; Franicola, D.; Dixon, T.; Frantz, M.-C.; Wipf, P.; Tyurina, Y.; Kagan, V. E.; Wang, H.; Greenberger, J. S. Two strategies for the development of mitochondrion-targeted small molecule radiation damage mitigators. *Int. J. Radiat. Oncol., Biol., Phys.* **2011**, *80*, 860−868.

(15) Shinde, A.; Berhane, H.; Rhieu, B. H.; Kalash, R.; Xu, K.; Goff, J.; Epperly, M. W.; Franicola, D.; Zhang, X.; Dixon, T.; Shields, D.; Wang, H.; Wipf, P.; Parmar, K.; Guinan, E.; Kagan, V.; Tyurin, V.; Ferris, R. L.; Zhang, X.; Li, S.; Greenberger, J. S. Intraoral mitochondrial-targeted GS-nitroxide, JP4-039, radioprotects normal tissue in tumor-bearing radiosensitive Fancd2(−/−) (c57bl/6) mice. *Radiat. Res.* **2016**, *185*, 134−150.

(16) Ji, J.; Kline, A. E.; Amoscato, A.; Samhan-Arias, A. K.; Sparvero, L. J.; Tyurin, V. A.; Tyurina, Y. Y.; Fink, B.; Manole, M. D.; Puccio, A. M.; Okonkwo, D. O.; Cheng, J. P.; Alexander, H.; Clark, R. S. B.; Kochanek, P. M.; Wipf, P.; Kagan, V. E.; Bayir, H. Lipidomics identifies cardiolipin oxidation as a mitochondrial target for redox therapy of brain injury. *Nat. Neurosci.* **2012**, *15*, 1407−1413.

(17) Ji, J.; Baart, S.; Vikulina, A. S.; Clark, R. S. B.; Anthonymuthu, T. S.; Tyurin, V. A.; Du, L.; St Croix, C. M.; Tyurina, Y. Y.; Lewis, J.; Skoda, E. M.; Kline, A. E.; Kochanek, P. M.; Wipf, P.; Kagan, V. E.; Bayir, H. Deciphering of mitochondrial cardiolipin oxidative signaling in cerebral ischemia-reperfusion. *J. Cereb. Blood Flow Metab.* **2015**, *35*, 319−328.

(18) Xun, Z.; Rivera-Sanchez, S.; Ayala-Pena, S.; Lim, J.; Budworth, H.; Skoda, E. M.; Robbins, P. D.; Niedernhofer, L. J.; Wipf, P.; McMurray, C. T. Targeting of XJB-5-131 to mitochondria suppresses oxidative DNA damage and motor decline in a mouse model of huntington's disease. *Cell Rep.* **2012**, *2*, 1137−1142.

(19) Escobales, N.; Nunez, R. E.; Jang, S.; Parodi-Rullan, R.; Ayala-Pena, S.; Sacher, J. R.; Skoda, E. M.; Wipf, P.; Frontera, W.; Javadov, S. Mitochondria-targeted ROS scavenger improves post-ischemic recovery of cardiac function and attenuates mitochondrial abnormalities in aged rats. *J. Mol. Cell. Cardiol.* **2014**, *77*, 136−146.

(20) LogP values were calculated with Instant JChem 15.8.31.0 (ChemAxon; http://www.chemaxon.com).

(21) Sprachman, M. M.; Wipf, P. A bifunctional dethylsulfoxide substitute enhances the aqueous solubility of small organic molecules. *Assay Drug Dev. Technol.* **2012**, *10*, 269−277.

(22) Skoda, E. M.; Sacher, J. R.; Kazancioglu, M. Z.; Saha, J.; Wipf, P. An uncharged oxetanyl sulfoxide as a covalent modifier for improving aqueous solubility. *ACS Med. Chem. Lett.* **2014**, *5*, 900−904.

(23) Xiao, J.; Weisblum, B.; Wipf, P. Trisubstituted (*E*)-alkene dipeptide isosteres as *β*-turn promoters in the gramicidin S cyclodecapeptide scaffold. *Org. Lett.* **2006**, *8*, 4731−4734.

(24) Nair, R. V.; Baravkar, S. B.; Ingole, T. S.; Sanjayan, G. J. Synthetic turn mimetics and hairpin nucleators: Quo vadimus? *Chem. Commun.* **2014**, *50*, 13874−13884.

(25) Beck, J. G.; Chatterjee, J.; Laufer, B.; Kiran, M. U.; Frank, A. O.; Neubauer, S.; Ovadia, O.; Greenberg, S.; Gilon, C.; Hoffman, A.; Kessler, H. Intestinal permeability of cyclic peptides: Common key backbone motifs identified. *J. Am. Chem. Soc.* **2012**, *134*, 12125−12133.

(26) Gray, R. A.; Vander Velde, D. G.; Burke, C. J.; Manning, M. C.; Middaugh, C. R.; Borchardt, R. T. Delta-sleep-inducing peptide: Solution conformational studies of a membrane-permeable peptide. *Biochemistry* **1994**, *33*, 1323−1331.

(27) Xiao, J.; Weisblum, B.; Wipf, P. Electrostatic versus steric effects in peptidomimicry: Synthesis and secondary structure analysis of gramicidin S analogues with (*E*)-alkene peptide isosteres. *J. Am. Chem. Soc.* **2005**, *127*, 5742−5743.

(28) Frantz, M.-C.; Pierce, J. G.; Pierce, J. M.; Kangying, L.; Qingwei, W.; Johnson, M.; Wipf, P. Large-scale asymmetric synthesis of the bioprotective agent JP4-039 and analogs. *Org. Lett.* **2011**, *13*, 2318−2321.

(29) Di, L. Strategic approaches to optimizing peptide ADME properties. *AAPS J.* **2015**, *17*, 134−143.

(30) Yagoda, N.; von Rechenberg, M.; Zaganjor, E.; Bauer, A. J.; Yang, W. S.; Fridman, D. J.; Wolpaw, A. J.; Smukste, I.; Peltier, J. M.; Boniface, J. J.; Smith, R.; Lessnick, S. L.; Sahasrabudhe, S.; Stockwell, B. R. RAS-RAF-MEK-dependent oxidative cell death involving voltage-dependent anion channels. *Nature* **2007**, *447*, 865−869.

(31) Skouta, R.; Dixon, S. J.; Wang, J.; Dunn, D. E.; Orman, M.; Shimada, K.; Rosenberg, P.; Lo, D.; Weinberg, J.; Linkermann, A.; Stockwell, B. R. Ferrostatins inhibit oxidative lipid damage and cell death in diverse disease models. *J. Am. Chem. Soc.* **2014**, *136*, 4551−4556.